Mast cells participate in smooth muscle cell reprogramming and atherosclerotic plaque calcification

Skenteris, N.T.; Hemme, E.; Delfos, L.; Karadimou, G.; Karlöf, E.; Lengquist, M.; ... ; Bot, I. Matic, L.

Vascular Pharmacology 150 (2023) 107167

Contents lists available at ScienceDirect

Vascular Pharmacology

journal homepage: www.elsevier.com/locate/vph

Mast cells participate in smooth muscle cell reprogramming and atherosclerotic plaque calcification

Nikolaos T. Skenteris [a,b,c], Esmeralda Hemme [d], Lucie Delfos [d], Glykeria Karadimou [b], Eva Karlöf [b], Mariette Lengquist [b], Malin Kronqvist [b], Xiang Zhang [b], Lars Maegdefessel [a,e], Leon J. Schurgers [f,g], Hildur Arnardottir [a], Erik A.L. Biessen [c], Ilze Bot [d], Ljubica Matic [b,*]

[a] Cardiovascular Medicine, Department of Medicine, Karolinska Institute, Stockholm, Sweden
[b] Vascular Surgery, Department of Molecular Medicine and Surgery, Karolinska Institute and Karolinska University Hospital, Stockholm, Sweden
[c] Department of Pathology, Cardiovascular Research Institute Maastricht (CARIM), Maastricht University Medical Centre, The Netherlands
[d] Division of BioTherapeutics, Leiden Academic Centre for Drug Research, Leiden University, The Netherlands
[e] Technical University Munich, Klinikum rechts der Isar, Department for Vascular and Endovascular Surgery, Germany
[f] Department of Biochemistry and CARIM, School for Cardiovascular Diseases, Maastricht University, The Netherlands
[g] Institute of Experimental Medicine and Systems Biology, RWTH Aachen University, Aachen, Germany

ARTICLE INFO

Keywords:
Atherosclerotic plaques
Mast cells
Smooth muscle cells
Intimal calcification
Biobank of Karolinska endarterectomy (BiKE)

ABSTRACT

Background: Calcification, a key feature of advanced human atherosclerosis, is positively associated with vascular disease burden and adverse events. We showed that macrocalcification can be a stabilizing factor for carotid plaque molecular biology, due to inverse association with immune processes. Mast cells (MCs) are important contributors to plaque instability, but their relationship with macrocalcification is unexplored. With a hypothesis that MC activation negatively associates with carotid plaque macrocalcification, we aimed to investigate the link between MCs and carotid plaque vulnerability, and study MC role in plaque calcification *via* smooth muscle cells (SMCs).

Methods: Pre-operative computed tomography angiographies of patients ($n = 40$) undergoing surgery for carotid stenosis were used to characterize plaque morphology. Plaque microarrays (n = 40 and $n = 126$) were used for bioinformatic deconvolution of immune cell populations. Tissue microarrays ($n = 103$) were used to histologically validate the contribution of activated and resting MCs in plaques.

Results: Activated MCs and their typical markers were negatively correlated with macrocalcification. The ratio of activated *vs.* resting MCs was increased in low-calcified plaques from symptomatic patients. There was no modulating effect of medication on MC ratios. *In vitro* experiments showed that SMC calcification attenuated MC activation, while both active and resting MCs stimulated SMC calcification and induced dedifferentiation towards a pro-inflammatory-, osteochondrocyte-like phenotype, without modulating their migro-proliferative function.

Conclusions: Integrative analyses from human plaques showed that MC activation is inversely associated with macrocalcification and positively with parameters of plaque vulnerability. Mechanistically, MCs induce SMC osteogenic reprograming, while matrix calcification in turn attenuates MC activation, offering new therapeutic avenues for exploration.

1. Introduction

Beyond hypercholesterolemia, solid experimental and clinical research has shown that inflammation drives atherogenesis [1]. Atherosclerotic plaques are characterized by a fibrous cap composed of smooth muscle cells (SMCs) and a lipid-rich necrotic core, along with intraplaque neovascularization, calcification and an ongoing inflammation with a repertoire of immune cells like macrophages, T-cells and

Abbreviations: CALC, Calcification; CEA, Carotid endarterectomy; CTA, Computed tomography angiography; CVD, Cardiovascular disease; IPH, Intraplaque hemorrhage; LRNC, Lipid-rich necrotic core; MC, Mast cell; SMC, Smooth muscle cell; TMA, Tissue microarray.

* Corresponding author at: Division of Vascular Surgery, Department of Molecular Medicine and Surgery, BioClinicum J8:20, Karolinska Institutet, SE-171 76 Stockholm, Sweden.
E-mail address: Ljubica.Matic@ki.se (L. Matic).

https://doi.org/10.1016/j.vph.2023.107167
Received 31 January 2023; Received in revised form 14 March 2023; Accepted 19 March 2023
Available online 21 March 2023

mast cells (MCs) [2,3]. Inflammation-mediated plaque calcification is the key feature of advanced human lesions resulting from formation of calcification nodules, yet its mechanistic impact on clinical events such as stroke or myocardial infarction is poorly understood [4,5]. We previously reported that molecular processes related to ossification are upregulated in carotid plaques from asymptomatic patients and patients on cholesterol-lowering therapy [6], while another large meta-analysis confirmed that carotid plaques from symptomatic patients contain less calcification than those from asymptomatic patients [6,7]. In recent years, the clinical need for non-invasive detection of vascular calcification to facilitate prediction of atherosclerosis progression and adverse events, has driven intensive research by our group and others in software developments based on computed tomography angiography (CTA) imaging, leading to a better resolution in structural and morphological assessment of plaque calcification [8,9].

Atheroprogression encompasses simultaneous development of micro- and macrocalcifications, but the molecular mechanisms and the cellular interplay engaging both immune cells and SMCs are still not entirely understood in carotid plaques. Emerging research in coronary plaques has shown that microcalcifications exacerbate plaque inflammation by stimulating the release of pro-inflammatory cytokines and chemokines [5], which have detrimental effects on plaque progression and stability [10] in humans [11] and mice [12]. Conversely, macrocalcifications are predominantly observed in late-stage plaques and research from our group has shown that they are surprisingly associated with suppressed inflammation, healing and carotid plaque stabilization processes on molecular level [9,13,14]. In particular, we showed surprisingly that highly calcified carotid plaques contained more quiescent SMCs as well as resting and anti-inflammatory immune cells, whereas activated immune cells were more abundant in low-calcified plaques [9,13]. SMCs display broad phenotypic plasticity in response to factors present in the atherosclerotic milieu and can undergo various forms of transdifferentiation, including an osteo-chondrogenic gene expression program. While upregulation of *SOX9* and *SMAD3* transcription factors induces osteogenic SMC transformation [15], we showed recently that the macrocalcified extracellular matrix in turn enables SMCs to restore a gene expression profile resembling a more differentiated, quiescent phenotype [14]. Interestingly, this inverse association of activated *vs.* quiescent SMCs, as well as activated *vs.* resting immune cells with macrocalcification, pertained even in plaques from symptomatic patients, a notion that has not been investigated so far.

MCs are among the key immune effectors in atheroprogression, since they release not only the MC-specific neutral proteases tryptase and chymase upon activation, but also a whole array of mediators such as histamine, cathepsins, growth factors, cytokines and chemokines [16,17]. Activated MCs are commonly found in the shoulder regions and particularly at the sites of erosion or rupture in coronary atherosclerotic lesions, *i.e.* in patients who died from myocardial infarction [18–20]. In addition, human studies have revealed an association of MCs with plaque neovascularization and hemorrhage that increase the risk of adverse events [21–23]. Experimental studies in animals have generally illuminated the crucial role of MCs in atheroprogression and plaque vulnerability [24,25]. However, the specific connection between MC activation and carotid plaque macrocalcification [26], recently identified from our human studies based on the large Biobank of Karolinska Endarterectomies (BiKE) [9], has not yet been reported.

The purpose of this study was to investigate the association between MC activation and plaque macrocalcification directly in the human disease, followed by exploration of the underlying interplay between MCs and SMCs in calcification. One of the challenges in the field of MCs biology, which has prevented similar human studies before, is that minor cell types like MCs are typically under-appreciated in a highly heterogeneous plaque tissue. To this end, we applied single-cell resolution bioinformatic methods by deconvolving the immune cell proportions, and particularly activated *vs.* resting MCs, from global transcriptomic data of human carotid plaques belonging to BiKE. We associated these MC phenotypes with plaque calcification and other morphological features from advanced CTA image analyses, as well as patient clinical data and medication. Histological and *in vitro* studies were also performed to validate and understand the mechanisms between MC activation and SMC transformation in calcification. Our large-scale human studies revealed that MC activation is inversely coupled to plaque macrocalcification and plays a role in SMC phenotypic modulation in response to inflammation **(Graphical Abstract)**.

2. Materials and methods

Additional material and methods are described in detail in the **Supplementary Material**.

2.1. Ethical statements

This study was done on subcohorts of patients enrolled in the **Bi**obank of **K**arolinska **E**ndarterectomy (**BiKE**). All human samples were collected with informed consent from patients or organ donors' guardians, as part of the ordinary medical and surgical procedures that do not put the patients at additional risk. All studies in BiKE have been approved by the Ethical Committee of Stockholm (official name of the ethical review board in Swedish "Regionala etikprövningsnämnden i Stockholm"). BiKE studies follow the guidelines of the Declaration of Helsinki. Studies were approved by the regional Ethical Committee with the following ethical permit numbers: DNr 02–147; 2009/295–31/2; 2011/950–32; 2013/2137–32; 2017/508–32; 2018/954–32; 2020/00274; 2012/619–32; 2009/512–31/2. BiKE ethical permits cover: all patients longitudinally collected over the years, including the subset of patients used in this particular study; both collection and actual research use of all biomaterials, imaging and patient data; collection and research use of normal control material from organ donors. The individual human data underlying this article cannot be shared publicly due to the General Data Protection Regulation (GDPR) and ethics laws that regulate the privacy of individuals that participated in the study. The microarray datasets used in the study are publicly available from Gene Expression Omnibus (accession numbers GSE21545 and GSE125771). Other data will be shared pertaining a reasonable request to the corresponding author.

In all animal experiments, mice were euthanized by cervical dislocation and no anaesthesia was used. To obtain bone marrow for the bone marrow derived mast cell culture, femurs and tibias were collected. The animal work was performed in compliance with the guidelines by the European Union Directive 2010/63EU and the Dutch Government, and was approved by the Animal Welfare Body of Leiden University.

2.2. Human carotid atherosclerosis cohort

2.2.1. BiKE cohort

Patients undergoing surgery for high-grade (>50% NASCET) [27] carotid stenosis at the Department of Vascular Surgery, Karolinska University Hospital, Stockholm, Sweden were consecutively enrolled in the study and clinical data recorded on admission. Symptoms (S) were defined as transitory ischemic attack (TIA), minor stroke (MS) and *amaurosis fugax* (AFX, retinal TIA). Patients without qualifying symptoms within 6 months prior to surgery were categorized as asymptomatic (AS) and indication for carotid endarterectomy (CEA) based on results from the Asymptomatic Carotid Surgery Trial (ACST) [28]. Patient medication encompassed cholesterol-lowering (ezetimib, HMG-CoA reductase inhibitors), anti-diabetics (metformin, insulin), anti-coagulants (warfarin, novel oral anti-coagulants) and anti-hypertensives (ACE inhibitors, calcium antagonists, beta-blockers, diuretics, angiotensin II blockers). Of note, none of the patients received MC stabilizers (eg. cromolyn sodium or pemirolast potassium). Carotid endarterectomies (carotid atherosclerotic plaques) were collected at surgery and retained within BiKE. The study cohort demographics,

details of sample collection and processing and transcriptomic analyses by microarrays were previously described in details [6,29,30]. Briefly, plaques were divided transversally at the most stenotic part; the proximal half of the lesion was used for RNA preparation while the distal half was immediately fixed in 4% formaldehyde for 48 h. Non-atherosclerotic, further referred to as normal artery, control samples (n = 10 in total) were obtained from macroscopically disease-free iliac arteries, from organ donors without any history of cardiovascular disease.

2.2.2. Computed tomography angiography (CTA) image analysis

Carotid plaques were assessed in pre-operative CTAs at the admitting hospital, using site-specific image acquisition protocols between March 2008 and October 2013 and a novel semi-automated, histopathologically validated software vascuCAP® (Elucid Bioimaging Inc., Boston, MA) as previously described [31]. Technical details of the software and its analysis algorithm have been described previously, including the approach taken for histologically validated quantification of CALC, LRNC and IPH [31,32]. Briefly, the software reconstructs CTA images (0.625 mm thick) and creates 3D segmentations with improved resolution and soft *vs.* hard tissue plaque component differentiation. A patient specific 3D point spread function restores image intensities and enables discrimination of tissue types such as LRNC and IPH. CTA images were analyzed in a blinded fashion by one observer (author E.K) using the vascuCAP® software. The software then interprets the Hounsfield units (HU) of adjacent voxels by maximising criteria that mimic the ground truth (*i.e.* expert annotated histology). The analysis provides a semi-automatically generated calcium volume of carotid plaques, which was analyzed with a threshold of 400 HU for calcification and a ratio was calculated (Vcalc/Vtot = calcification degree). Overall, the following measurements were computed from each single plaque: (1) geometry, including the total plaque volume, maximum percentage of stenosis according to the diameter and cross-sectional area, maximum cross-sectional dilation according to the luminal diameter and luminal area, maximum cross-sectional luminal area/wall area ratio, and plaque burden ratio as measured by the cross-sectional wall area or wall volume divided by vessel area or vessel volume, respectively; and (2) tissue composition in two dimensions at the region of maximum stenosis (maximum CALC area, maximum IPH area, maximum LRNC area) and in three dimensions (CALC, IPH, LRNC volumes), and their corresponding proportions relative to the total vessel volume [33]. We have utilized and more extensively described the practical use of this software in recent publications from the BiKE biobank [9,13,34].

2.3. Study subcohorts

Several subcohorts from BiKE were used in this study, as illustrated in **Fig. S1**. For clarification, low *vs.* high calcified plaques (n = 40) were used for transcriptome profiling and for further deconvolution assessment for estimation of immune cell fractions. Carotid lesions of the same patients (n = 40) were assessed with CTA and the images were further processed with vascuCAP software for quantification of morphological characteristics **(Fig. S1A and S1B)**. This subcohort from BiKE was described in detail in the following publications [9,13] and used here for discovery. Plaques of n = 126 additional patients and n = 10 normal arteries were also microarray profiled, whereas plaques of n = 18 non-overlapping patients were processed for proteomics with liquid chromatography – mass spectrometry (LC-MS/MS) **(Fig. S1C)**. These two non-overlapping subcohorts were used for transcriptomic and proteomic validation and further investigation of the discovery data in the context of more general atherosclerosis (not only with focus on calcification) and also previously described in detail [6,35]. Plaques of additional n = 103 patients were used for the construction of tissue microarrays (TMAs) for histological validation **(Fig. S1D)**, as described previously [30,35]. Low *vs.* high calcified lesions (n = 6) were used for gross immunohistochemistry **(Fig. S1E)**. Finally, low *vs.* high calcified lesions (n = 6) were used for *ex vivo* and *in vitro* investigations **(Fig. S1F)**.

2.4. Statistical analyses

Normal distribution of the data was assessed using the Shapiro-Wilks normality test. Comparative statistics between normally distributed groups was performed using Student's t-test or one-way ANOVA multiple comparison test. The Kruskal–Wallis multiple comparison one-way ANOVA or Mann–Whitney t-test were used when normal distribution assumption was invalid. Spearman and Pearson correlation coefficient were used to assess all correlations according to normality test result. Multivariable linear regression analysis was used to estimate the significance between activated MC fraction and plaque morphological features from CT assessment. Differences between groups were considered significant at P values <0.05. All statistical analyses were performed with GraphPad Prism 9.0 (GraphPad Software, Inc., San Diego, CA, USA).

3. Results

3.1. Mast cells associate with plaque vulnerability features

Pre-operative CTA images from patients undergoing CEA (n = 40 totally) were analyzed for the extent of CALC, LRNC, IPH and other plaque morphological features. Matched carotid plaques were analyzed for global gene expression by microarrays [9] and immune cell proportions were estimated from these bulk microarrays using deconvolution by the CIBERSORT software [36] (Fig. 1A**)**. For clarification, cell populations in the referred publication were defined using an *in vitro* validated list of cell-specific signature markers, consisting of totally 547 genes **(Table S1)**, here used for estimating the relative proportions of all 22 immune cell populations [36]. According to this, MC population was generally characterized by the high expression of markers such as *TRIB2*, *CMA1*, *CPA3*, *CST7*, *CTSG*, *ELANE*, *FCER1A*, *HDC*, *HPGDS*, *TPSAB1* and *MS4A2*. MC activation was specifically characterized by higher mRNA expression of cytokines such as *IL1A*, *CCL1*, *CCL20*, *CCL4*, *CCL5*, *CCL7*, *CCL8*, *CXCL3*, *CXCL5*, as well as markers such as *CD33*, *CD37*, *CD38*, *CD69*, *CLEC7A*, *CSF2*, typically upregulated immediately upon activation [36–38].

Our analysis confirmed the presence of MCs in plaques, with mean ± SD percentage of 2.6 ± 3.6% resting and 4.8 ± 4.8% activated MCs of the total immune cell content in the whole discovery subcohort, containing n = 22 less calcified (0–10% CALC content) and n = 18 more calcified plaques (16–60%). Plaques were then stratified with respect to CALC content into two well-separated groups of the 10 low-calcified (0–3% CALC) *vs.* the 10 high-calcified plaques (30–60%) from the whole discovery subcohort (Fig. 1B**)**. The average percentage of both MC populations in the total immune cell content in low-calcified plaques was estimated to be 3.1 ± 3.5% (1.7 ± 2.2% resting and 4.3 ± 4.2% activated), while in the high-calcified plaques it was 3.2 ± 3.5% (4.8 ± 3.4% resting and 1.5 ± 2.8% activated). These results revealed a significant abundance of resting MCs in high-calcified plaques, whereas low-calcified plaques contained relatively more activated MCs (Fig. 1C**)**, a finding that validated our previous results [9]. Multivariable correlation analysis between MCs and volume proportions of CALC, IPH and LRNC, showed that activated MCs were independently negatively correlated with CALC (Fig. 1D), whereas they positively correlated with IPH in a univariate analysis **(Fig. S2A)**. In addition, univariate analysis showed a negative correlation between activated MCs and max stenosis by area and diameter, as well as plaque burden volume **(Fig. S2B)**. Together, these initial studies connecting clinical imaging and cellular plaque analysis, showed that MC activation is negatively associated with macrocalcification and positively with IPH.

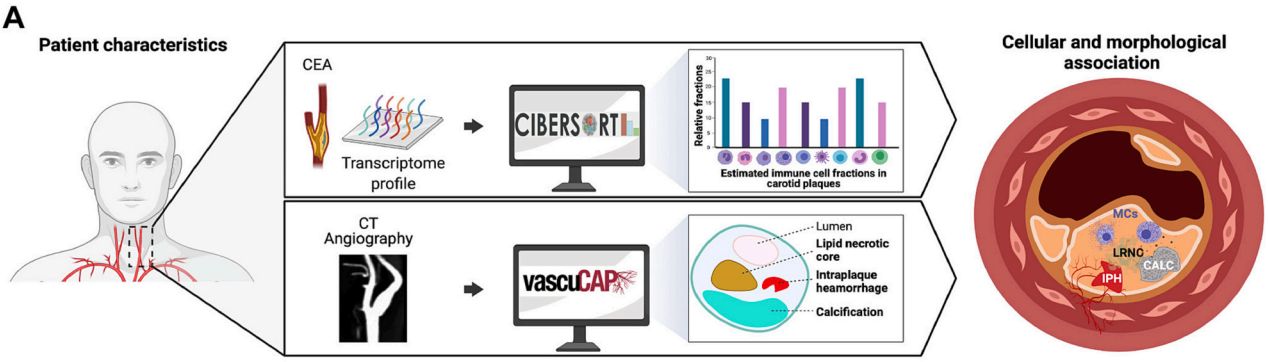

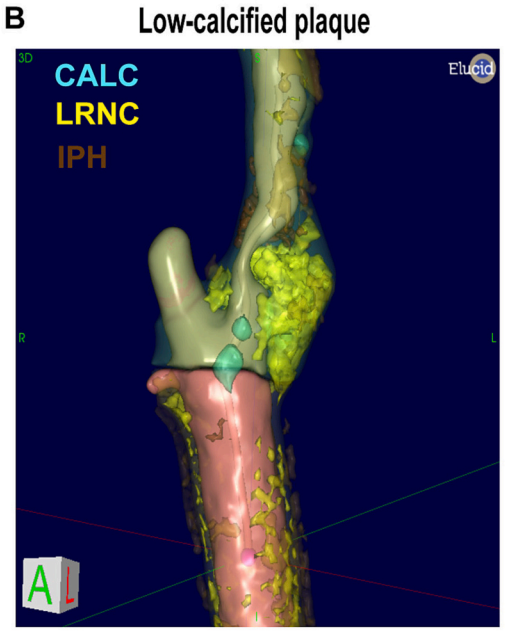

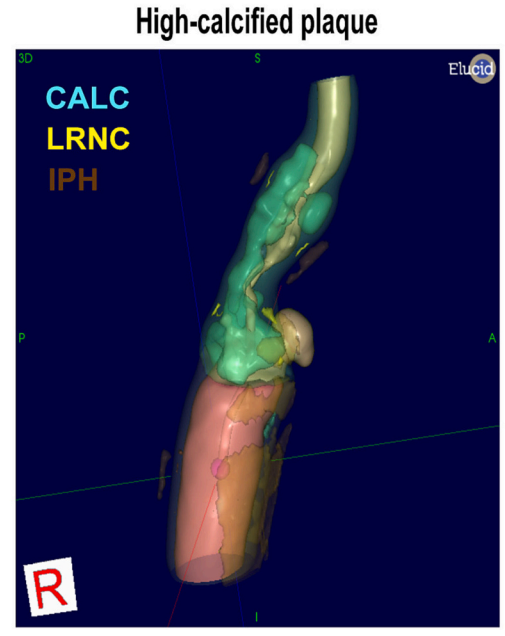

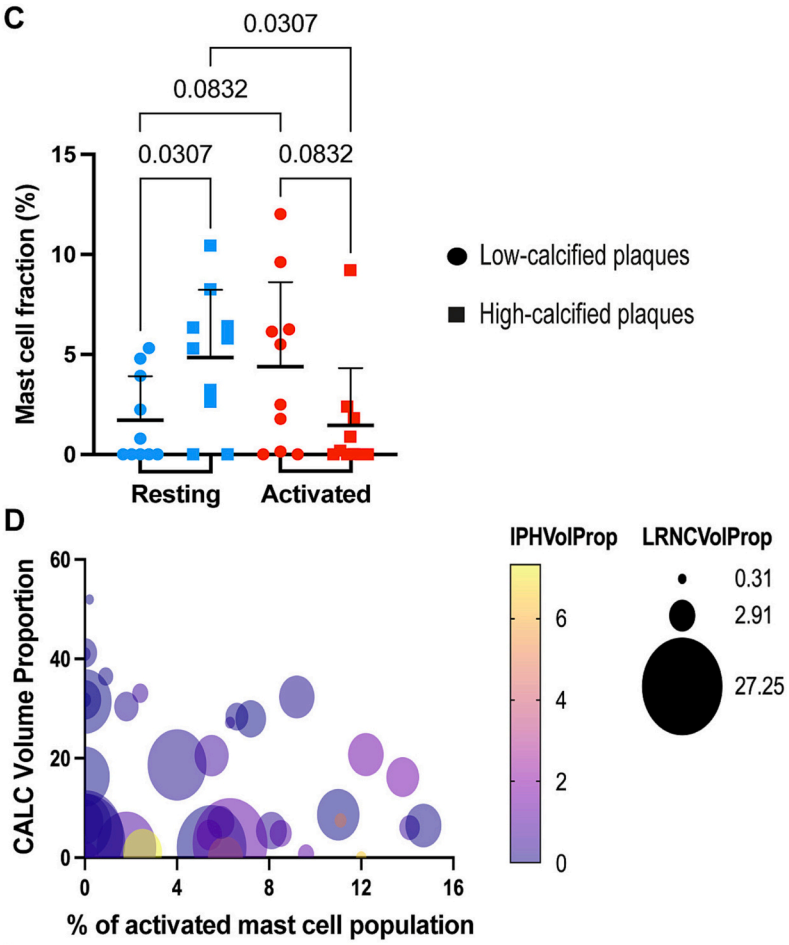

Variable	Estimate	Standard error	95% CI	|t|	P-value
Intercept	8.224	1.907	4.356 to 12.09	4.312	<0.001
CALCVolProp	**-0.1272**	**0.06216**	**-0.2533 to -0.001185**	**2.047**	**0.048**
IPHVolProp	-0.08111	0.4658	-1.026 to 0.8636	0.1741	0.863
LRNCVolProp	-0.2160	0.1168	-0.4528 to 0.02087	1.849	0.073
R squared = 0.16					

(caption on next page)

Fig. 1. Activated mast cells associate with key plaque morphological features.
A) Workflow of the deconvolution methodology applied in the study. Diagnostic CT angiographies of carotid atherosclerotic plaques were analyzed with the histologically validated vascuCAP software for evaluating plaque calcification and other morphological features. Plaques were profiled with global transcriptomics using microarrays. A computational deconvolution method by public CIBERSORT software was then applied to enumerate immune cell fractions from bulk plaque gene expression profiles. **B)** 3D reconstructive images of low- and high-calcified carotid plaques from CT analysed with VascuCAP software, where colored components represent the following plaque features: CALC (turquoise), LRNC (yellow) and IPH (brown). **C)** Resting and activated MC fractions enrichment in plaques stratified by degree of calcification ($n = 20$ total; $n = 10$ low-calcified *vs* n = 10 high-calcified). Kruskal–Wallis multiple comparison one-way analysis; data expressed as mean with SD. **D)** Multiple linear regression analysis between activated MC fraction and CALCVolProp, LRNCVolProp and IPHVolProp as estimated by vascuCAP analysis ($n = 40$). The graph is complemented by the table with more detailed statistical analysis. Differences between groups were considered significant at $P < 0.05$. (For interpretation of the references to colour in this figure legend, the reader is referred to the web version of this article.)

3.2. Mast cell activation in plaques is not attenuated by medication

The presence of macrocalcification, as a stabilizing factor for carotid plaques, may be a result of medication, particularly cholesterol-lowering therapy. Statin use has been associated with plaque remodeling processes, depicted by the enrichment of calcification [9,39]. Here, we employed TMAs for histological validation of MCs in plaques. TMAs are a large-scale histological method where plaques from many patients can be simultaneously analyzed in a standardized and mutually comparable way (thus called 'microarrays') [30,35]. Indeed, staining of TMAs from $n = 103$ patients with MC markers tryptase and chymase confirmed the presence of both MCs populations (resting and activated) in lesions. Histologically, MCs were classified as "resting" when the granules were compacted and maintained inside the cell, while "activated" when granules were found spread in the proximity of the cell (Fig. 2A) [21,40]. All MCs in plaques stained positive for tryptase, while some of the MCs contained chymase as well, as previously described [21,40]. The number of resting and activated MCs in lesions was quantified and normalized by tissue area (mm^2) [23]. Interestingly, stratification of the data according to medication showed that neither cholesterol-lowering, nor anti-diabetic, anti-coagulant or anti-hypertensive therapies had any beneficial effect on modifying the MC ratios in plaques (Fig. 2B).

3.3. Mast cell markers are enriched in low-calcified plaques, even in symptomatic patients

We also related MC activation (based on the granule localization) with other stainings from TMAs (evaluated by semi-quantification).

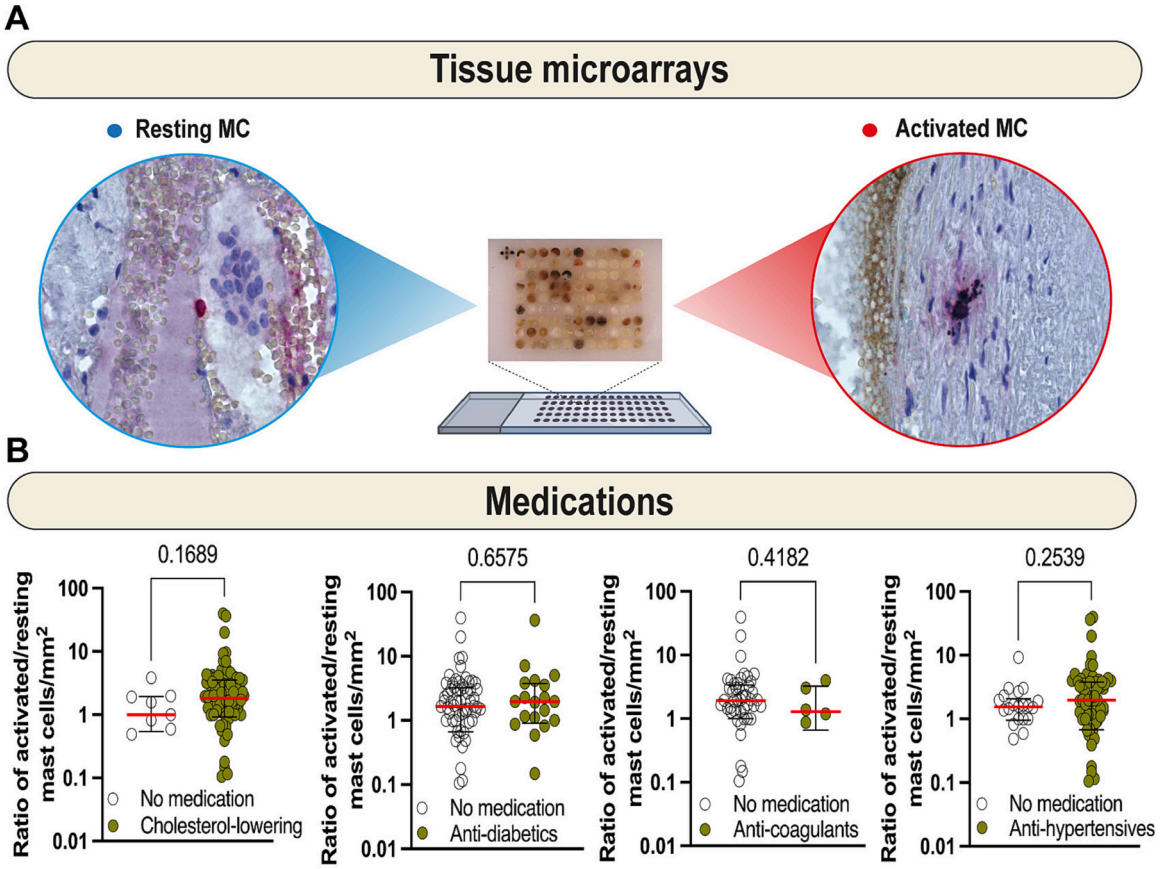

Fig. 2. Effect of patient medication on mast cell phenotype in plaques.
A) Tissue microarrays (TMAs) have been used to simultaneously analyze plaques from $n = 103$ patients for histological classification of resting (blue) *vs.* activated (red) MCs with tryptase (red) / chymase (green) staining, respectively. **B)** Quantified ratio of MC phenotypes per mm^2 of plaque section, stratified according to the patient medication: non-cholesterol-lowering ($n = 9$) *vs.* cholesterol-lowering ($n = 78$; *i.e.* ezetimib, HMG-CoA reductase inhibitors), non-anti-diabetics ($n = 67$) *vs.* anti-diabetics (n = 20; metformin, insulin), non-anti-coagulants ($n = 49$) *vs.* anti-coagulants (n = 6; warfarin, novel oral anti-coagulants), non-anti-hypertensives ($n = 22$) *vs.* anti-hypertensives ($n = 65$; ACE inhibitors, calcium antagonists, beta-blockers, diuretics, angiotensin II blockers). Statistical significance between groups was assessed by Mann–Whitney test; data expressed as median with interquartile range. Differences between groups were considered significant at $P < 0.05$. (For interpretation of the references to colour in this figure legend, the reader is referred to the web version of this article.)

Histological Alizarin Red and Perl's iron stainings for calcification and IPH respectively, validated the bioinformatic association with MCs in a multivariable analysis and confirmed that the total number of MCs independently negatively correlated with calcification (n = 103; P = 0.037) **(Fig. S3A)**. Activated MCs again showed a trend for negative correlation with calcification (n = 103; P = 0.054) **(Fig. S3B)**.

To further investigate the presence of markers and mediators associated with MCs in human plaques, we queried a non-overlapping, larger BiKE microarray dataset for a specific gene signature of MC activation [16,37,41]. The majority of typical activated MC markers, such as *CD63*, *CD69*, *KIT*, *CMA1*, *CPA3*, *TPSAB1*, *SRGN*, *CLEC7A*, were increased in lesions (n = 126) compared to normal arteries (n = 10) (Fig. 3A**)**, but also in plaques from symptomatic patients (n = 86) compared to asymptomatic ones (n = 40) (Fig. 3C**)**. In particular, *CD63* is expressed by several immune cell subsets such as macrophages, neutrophils, dendritic cells and platelets, however, extensive body of research in MCs has formed the notion that *CD63*, combined with other MC markers, can be used as an activation marker [42], since it is required for efficient IgE-mediated MC degranulation [43].

We also investigated this molecular signature of activated MCs specifically in transcriptomic data from plaques stratified by calcification (n = 40). Again, an enrichment of activated MC genes was found in low- *vs.* high-calcified plaques (Fig. 3B**)**, and even in low- (n = 10) *vs.* high- (n = 10) calcified plaques from symptomatic patients only (Fig. 3D). Similar results were obtained from plaque mass spectrometry data, where activated MC proteins were more abundant in plaques of symptomatic patients (n = 9) compared to asymptomatic ones (n = 9) **(Fig. S4A)**. The findings related to patient symptomatology were further evaluated by multivariable correlation analysis between activated MCs and morphological features of plaques from symptomatic patients (n = 20), where activated MCs again independently negatively correlated with CALC (**Fig. S4B**). Collectively, our data from BiKE revealed a robust and specific enrichment of activated MC gene signature in low-calcified plaques of symptomatic patients.

3.4. MCs induce matrix calcification via SMCs, which in turn attenuates MC activation

We next sought to investigate the environment surrounding MCs in plaques with special focus on SMCs, given that SMCs are the major cell type that undergoes phenotypic switching during vascular calcification [44]. Staining of plaques showed tryptase$^+$ cells in the proximity of calcified regions abundant of α-SMA$^+$ cells. Of interest, α-SMA coupled to the osteo-chondrogenic RUNX2 and SOX9 markers, showed that tryptase$^+$ activated MCs are found in fibrous cap, shoulder and necrotic core regions. Here, MCs were localized in proximity to α-SMA/SOX9$^+$ SMCs, both in low- and high-calcified plaques, and close to α-SMA/RUNX2$^+$ SMCs in high-calcified plaques, suggesting that these cells may play synergistic roles in macrocalcification **(Fig. S5)**.

Ex vivo supernatant transfer methods were utilized by culturing freshly collected low- and high-calcified plaques, as estimated from CTA images. The plaque medium was transferred onto bone marrow-derived MC culture (>98% MC purity), after which MC activation status was analyzed and visualized as percentage of CD63$^+$ cells of CD117$^+$FcεRI$^+$ (Fig. 4A, B**)**. In confirmation of our bioinformatic data, supernatants of highly calcified plaques did not induce MC activation and reduced

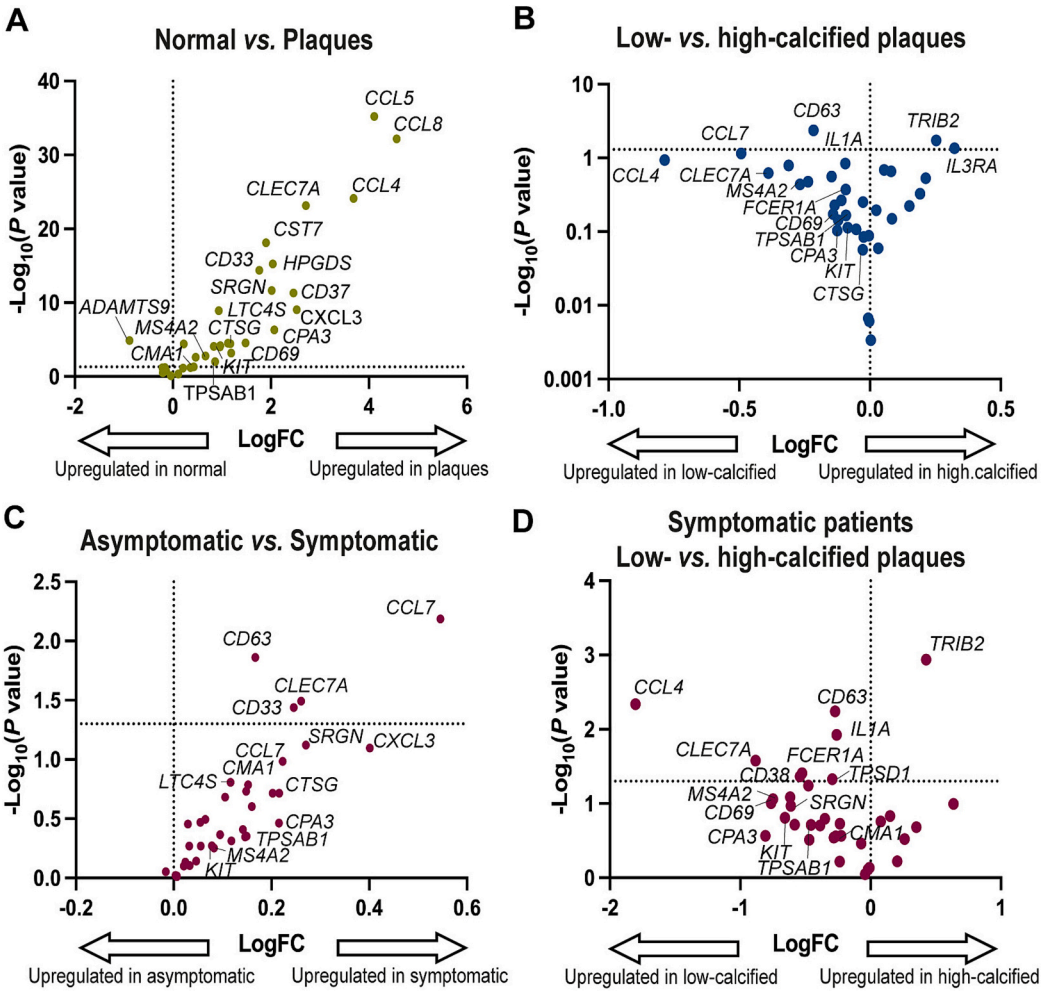

Fig. 3. Mast cell-specific gene signature expression in association with plaque calcification and patient symptoms.
A) Volcano plot of MC related genes expression in microarrays comparing normal arteries (n = 10) *vs.* plaques (n = 126). **B)** Volcano plot of MC related genes expression in microarrays comparing all low- (n = 22) *vs.* high- (n = 18) calcified plaques. **C)** Volcano plot of MC related genes expression in microarrays comparing plaques from asymptomatic (n = 40) *vs.* symptomatic (n = 86) patients. **D)** Volcano plot of MC related genes expression in microarrays comparing low- (n = 10) *vs.* high- (n = 10) calcified plaques from symptomatic patients only.

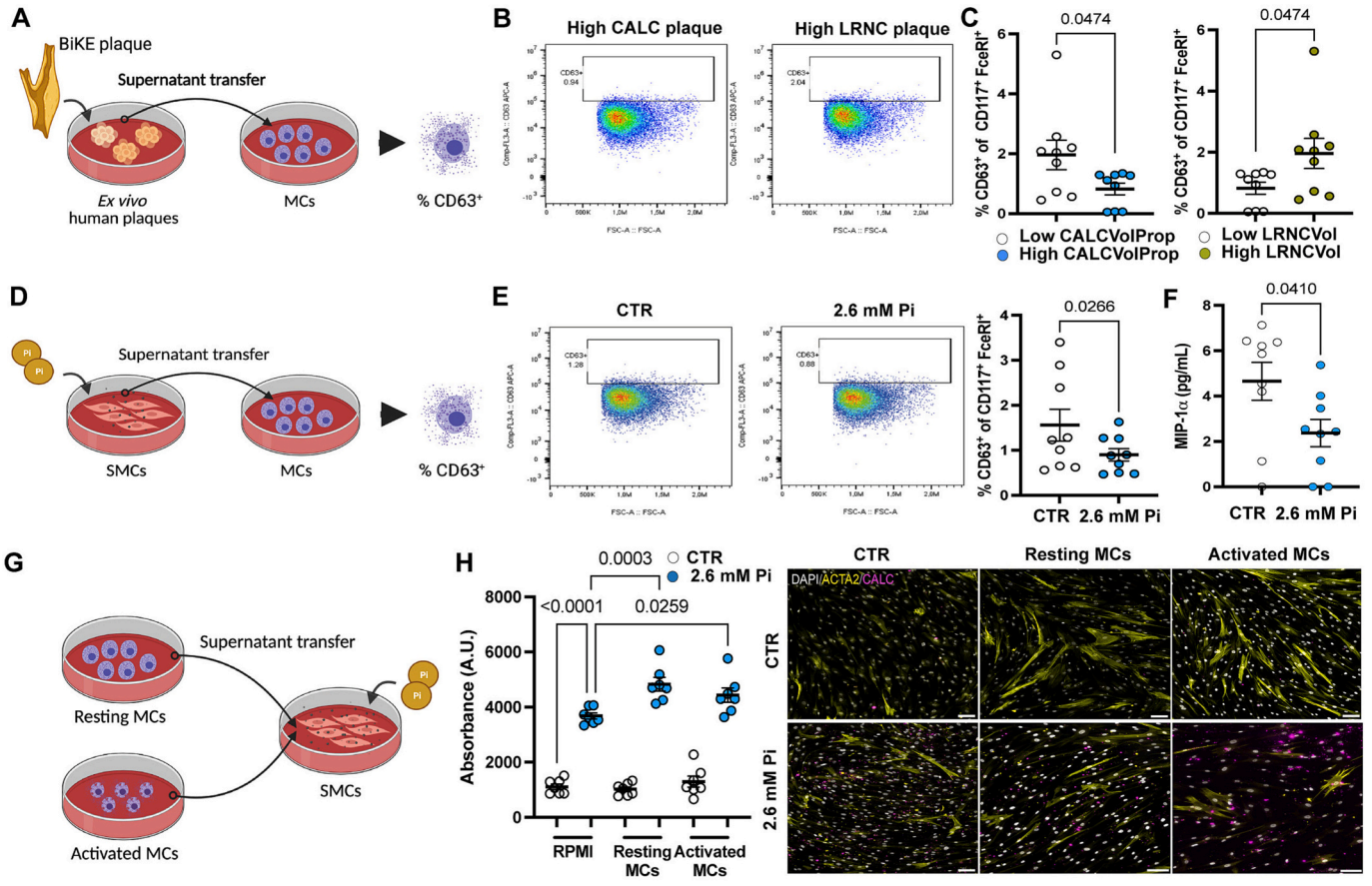

Fig. 4. Calcification inhibits mast cell activation, whereas both resting and activated mast cells induce smooth muscle cell calcification.
A) Schematic representation of atherosclerotic plaques cultured *ex vivo* for 24 h and supernatant transfer on bone marrow-derived MCs to assess their activation. **B)** Representative FACS plots show the percentage of $CD63^+$ cells of $CD117^+FcεRI^+$ for a high-calcified (CALC) plaque and a low calcified/high-lipid necrotic core (LRNC) plaque. **C)** Quantification of MC activation from the supernatants of atherosclerotic plaques clustered for calcification and lipid content (3 low *vs.* 3 high CALCVolProp and LRNCVol). Statistical significance between groups was assessed by Mann-Whitney *t*-test, data expressed as mean with SEM. **D)** Schematic representation of HAoSMC calcification assay with 2.6 mM Pi for 12 days and supernatant transfer on bone marrow-derived MCs to assess their activation. **E)** Quantification of MC activation from the supernatants of calcified HAoSMCs, illustrated in the representative FACS plots as the percentage of $CD63^+$ cells of $CD117^+FcεRI^+$. Primary cells from patient tissues were used in this experiment. Statistical significance between groups was assessed by paired Student's t-test, data expressed as mean with SEM. **F)** Quantification of mouse MIP-1α protein from the supernatants of MCs after supernatant transfer of calcified HAoSMCs for 12 days. Statistical significance between groups was assessed by Student's t-test; data expressed as mean with SEM. **G)** Schematic representation of supernatant transfer of bone marrow-derived MCs (resting or activated) on HAoSMCs and evaluation of their calcification in presence of 2.6 mM Pi for 12 days. **H)** Quantification of HAoSMC calcification with the use of OsteoImage™ mineralization assay after 12 days. Statistical significance between groups was assessed by one-way ANOVA multiple comparison test; data presented as mean with SEM. Representative images of the calcification assay where calcification was visualized by OsteoImage mineralization assay (magenta), HAoSMCs by ACTA2 antibody (yellow) and nuclei by DAPI (white). Scale bar 100 μm. All experiments were performed in triplicates. Differences between groups were considered significant at P values <0.05. (For interpretation of the references to colour in this figure legend, the reader is referred to the web version of this article.)

inflammatory MIP-1α secretion by MCs **(Fig. S6A)**, while supernatants from low-calcified plaques with large LRNC induced degranulation of MCs (Fig. 4C).

The direct connection between MCs and SMCs in calcification was explored *in vitro* (Fig. 4D). Supernatants of human aortic SMCs (HAoSMCs) calcified in 2.6 mM Pi for 12 days inhibited bone marrow-derived MC activation (Fig. 4E) and attenuated MIP-1α secretion (Fig. 4F), confirming our *ex vivo* results, while CD63 expression was absent in the resting MC cultures **(Fig. S6B)**. Of note, approximately 10% $CD63^+$ MC activation was reached using IgE stimulation as a positive control (as commonly observed in similar experiments by others), which was sufficient to induce the release of inflammatory cytokines and chemokines, such as TNFα, IL-6, MCP-1 (CCL2), MIP-1α(CCL3) and MIP-1β (CCL4) into the supernatant **(Fig. S6C)**. The low MC activation percentage *in vitro* corresponds well to the physiological situation in human plaques, yet leads to profound downstream effects. It is commonly accepted that this continuous, low grade MC activation provides a constant enhancement of the inflammatory response that aids plaque vulnerability. Based on the negative and positive controls (MC supplementation with inorganic Pi alone), a significant increase in MC activation was observed upon exposure to Pi stimulated SMC supernatant compared to Pi only **(Fig. S6D)**. Importantly, none of the experimental conditions affected cell viability (all >96%; **Fig. S6E**), confirming that the effects on MC activation were caused by SMC calcification process itself and not Pi only.

The reverse effect of supernatants from resting and activated MC cultures on the HAoSMC calcification was also tested *in vitro* (Fig. 4G). Supplementation of HAoSMCs grown in 2.6 mM Pi culture media for 12 days with supernatants from both resting and active MC, further increased the calcified nodules formation (Fig. 4H) compared to Pi only, suggesting that both MC populations could induce the extracellular matrix mineralization process. Searching for the possible mechanistic explanation of this effect, we re-analyzed the public dataset of the extracellular vesicles proteome from resting and activated bone marrow-

derived mouse MCs [45], which revealed that both cell phenotypes secrete distinct proteins related to the mineralization process (*i.e.* PRG4, DCN) **(Fig. S7A)**. Recent studies from our group showed that exogenous administration of PRG4 modulates osteogenic SMC differentiation [14], whereas others reported that DCN promotes arterial SMC calcification [46]. In addition, both MC populations secrete TGF-β implicated in calcification by modulating SMC phenotypic plasticity [47]. To validate the presence of TGF-β in the secretome of both resting and activated MCs, we quantified its protein levels in MC supernatants by ELISA **(Fig. S7B)**, suggesting that this particular cytokine may drive the osteogenic differentiation of SMCs under high Pi conditions as suggested before by others [48]. Taken together, these *in vitro* data show that MCs can induce SMC calcification independently of their phenotype, while subsequent SMC matrix calcification dampens MC activation in return.

3.5. Mast cells reprogram SMCs towards an osteochondrogenic phenotype

To mechanistically characterize the role of MCs in promoting SMC modulation under calcification conditions, we show that HAoSMCs cultured in high Pi supplemented with resting or active MC supernatants lose the expression of typical SMCs markers (*ACTA2*, *MYH11*, *CNN1*) already after 6 days and this repression was even stronger than in the case of Pi treatment alone **(**Fig. 5A**)**. Concomitantly, these HAoSMCs strongly upregulated osteochondrogenic markers *SOX9*, *SMAD3*, *BMP2*, whose expression remained elevated up to day 12 **(**Figs. 5A**, S8A and S8B)**. However, these HAoSMCs did not upregulate typical osteoblastic markers such as *RUNX2* and *ALPL* **(**Fig. 5A **and S8B)**, result which is in line with other published studies [49]. It has been shown that in high Pi conditions, *RUNX2* upregulates the transcription of downstream target genes that regulate bone development including *BMP2* [summarized by Chen et al. [50]] and downregulation of SMC lineage markers [51]. In addition, high Pi supplemented with MC supernatants induced a pro-inflammatory status in HAoSMCs in early stages up to day 6, as observed by the upregulation of *CD68* and *SPP1* that both were later repressed by day 12. Moreover, a distinct expression of *CCND1*, a cell cycle regulator reported to enable SMC reprograming towards a synthetic phenotype [52], was activated in this condition. This was indicated also by the decreased ACTA2 expression at protein level **(**Fig. 4H**)**, and no strong effects on apoptosis markers (*CASP3*).

Functionally, MC supernatants in combination with Pi induced secretion of IL-1β by HAoSMCs during the mineralization process **(**Fig. 5B **and S8C)**, but MC supernatants alone did not actually promote HAoSMCs migration or proliferation **(**Fig. 6A and B**)** [53]. This is congruent with the cytokine panel profiling of the supernatants from *ex vivo* cultured plaques, showing an upregulation for IL-1β and GM-CSF in high- compared to low-calcified plaques **(**Fig. 6C**)** [54]. Here again, similarly high levels of TGF-β were observed in both plaque supernatants, confirming our result obtained from both MC phenotypes, suggesting that TGF-dependent osteo-inductive signaling is involved in plaque calcification. Collectively, these data confirm that both resting and activated MC supernatants in combination with high Pi can induce a reprogramming of vascular SMCs towards an osteogenic phenotype **(Graphical Abstract)**.

4. Discussion

In this study, we present the first evidence for a role of MCs in vascular calcification, showing that activated MCs are prevalent in low-calcified carotid plaques, especially those from patients with symptoms, whereas resting MCs are abundant in high-calcified plaques. Both activated and resting MCs are capable of inducing SMC reprogramming and transition towards a pro-inflammatory, osteochondrocyte-like phenotype, while ectopic calcification ultimately suppresses MC activation.

Recent single-cell RNA sequencing data of mouse [55] and human [41] plaques confirmed the presence of a distinct population of MCs, however, single-cell studies are still done on a small number of samples and are not representative for the full spectrum of human plaque heterogeneity. With an aim to scale-up and enumerate the relative enrichment of MC populations in a large patient cohort, we applied bioinformatic microarray deconvolution method on BiKE carotid plaques stratified according to the degree of calcification. This analysis revealed that both MC fractions constitute about 8% (3% resting and 5% activated) of all plaque immune cells. Our previous publications reported an overall suppression of inflammatory pathways in high-calcified plaques [9], while here we extend that work to the estimation of active and resting MCs abundance in connection to plaque calcification. Histopathological studies conducted in human specimens have shown that activated MCs are present in ruptured plaques [19], especially in calcified [56] rupture-prone shoulder regions [18], associated with neovessels [21,23] and signs of hemorrhage and thrombosis [20,23], and similar was found in our study where IPH was assessed from CTA images. In addition, activated MCs promote angiogenesis under ischemia [57] and were sporadically associated with stippling and morula-type calcifications in human endarterectomies [26,56]. In support of our observations, research in aortic stenosis revealed that MCs colocalized with macrophages and neovessels mainly in the calcified regions of aortic valve leaflets [58,59] [60,61]. Of note, extracellular tryptase has been observed at sites where calcification process starts in the pineal gland, suggesting that MC activation could potentially contribute to the calcification process more generally in the body [62].

The association of MC phenotypes with patient symptomatology showed that activated MC gene signatures were consistently enriched in plaques compared to control arteries and particularly in plaques of symptomatic patients compared to asymptomatic ones [23,63]. These results are in line with previous research where MC abundance was associated with symptomatic carotid artery disease [64] and the incidence of future adverse events [23]. In extension, in our study the gene signature of activated MC was enriched even in comparison of low- *vs.* high-calcified plaques from symptomatic patients only, where low-calcified plaques are typically more lipid rich and vulnerable [9]. Another translational aspect of our study is the evaluation of MC phenotypes in association with patient medication. The majority of CVD patients receive cholesterol- and blood pressure- lowering drugs, anti-coagulant medication, and many of them also diabetes treatment considering the relationship between these diseases. Our data indicated that these medications do not significantly affect neither the MC abundance in plaques, nor their phenotype. Despite the reports that cholesterol-lowering drugs and warfarin (anti-coagulant) increase calcification and attenuate plaque vulnerability *via* reducing inflammation [6,39,65], they do not seem to exert their beneficial effects on MC phenotype conversion in atherosclerotic lesions. In line, reduced plasma total IgE levels were previously observed in patients receiving cholesterol-decreasers, without any concomitant effect on plaque MC numbers [66]. However, elevated IgE levels were associated with hyperlipidemia and CVD [67] and experimental administration of an anti-IgE antibody treatment reduced MC activation and plaque progression in mice [68]. Hence, a more MC-tailored, locally targeted intervention may prove beneficial, especially taking into account that the MC phenotype seems to be strongly influenced by the plaque microenvironment itself.

Considering that advanced calcified plaques are dominated by classical SMCs [9] and as shown here also resting MCs, we endeavored to explore this relationship. Our results have shown that supernatants from calcified conditions indeed attenuated MC degranulation and cytokine release, validating bioinformatic findings. In confirmation of the previously published studies, even though we did not show a direct association of MCs with plaque LRNC as evaluated by CTA or histology [17], supernatants from low-calcified plaques with large LRNC volume provoked MC degranulation *in vitro*. On the other hand, SMCs exposure to supernatants from both resting and activated MCs under high Pi conditions led to the downregulation of typical contractile SMC markers and switching towards the osteochondrogenic phenotype [44]. Such results

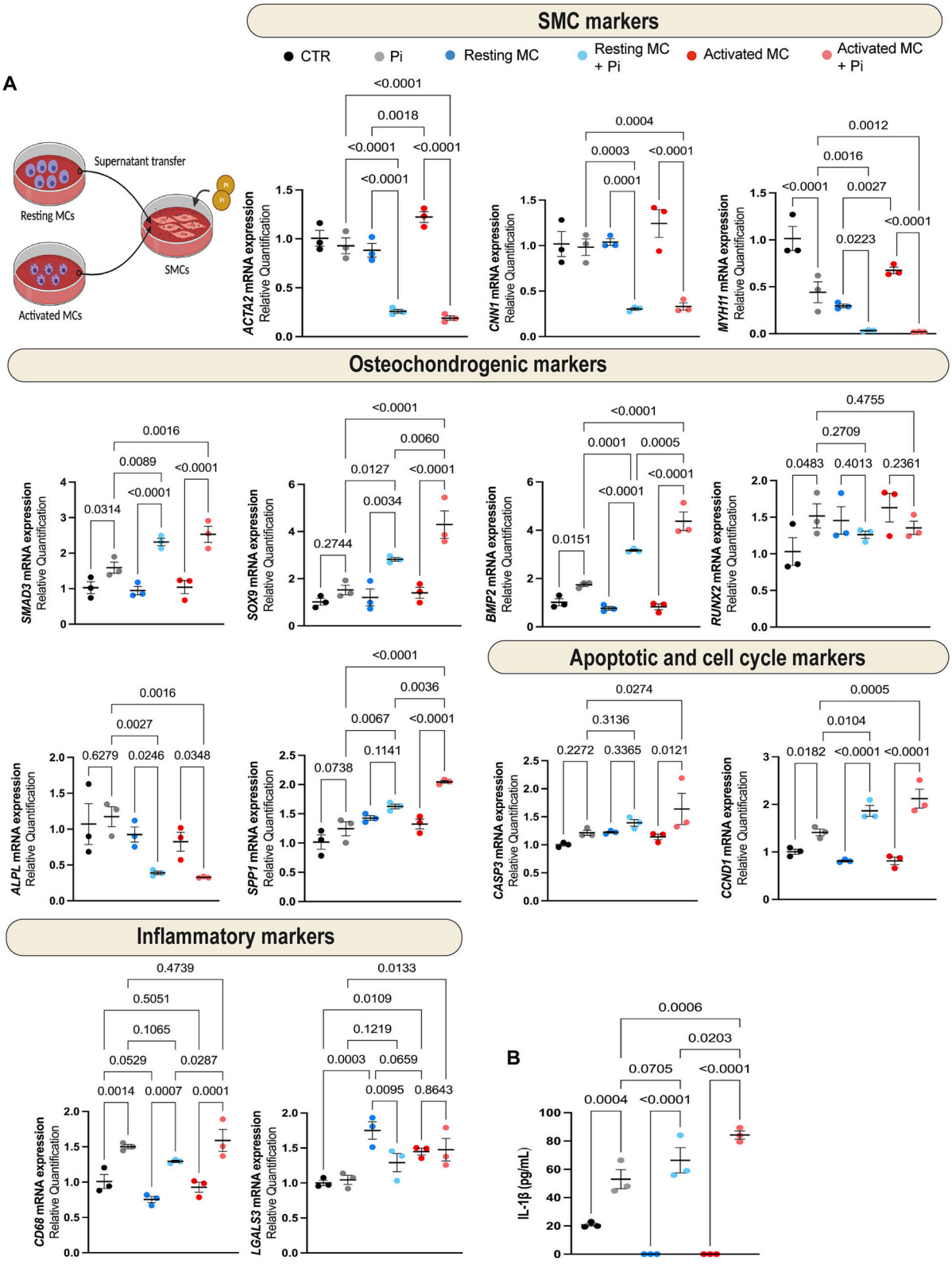

Fig. 5. Mast cells reprogram vascular smooth muscle cells towards an inflammatory, osteochondrogenic phenotype.
A) Gene expression analysis of typical contractile markers, osteochondrogenic, inflammatory and proliferation/apoptosis markers of HAoSMCs treated with 2.6 mM Pi and supernatant from resting or activated MCs for 6 days. Experiment was performed in biological triplicates. Statistical significance between groups was assessed by one-way ANOVA multiple comparison test; data expressed as mean with SEM. **B)** IL-1β protein quantification in the supernatants of the HAoSMCs treated with 2.6 mM Pi supplemented supernatant from resting or activated MCs for 6 days. Statistical significance between groups was assessed by one-way ANOVA multiple comparison test; data expressed as mean with SEM. All experiments performed in biological triplicates. Differences between groups were considered significant at *P* values <0.05.

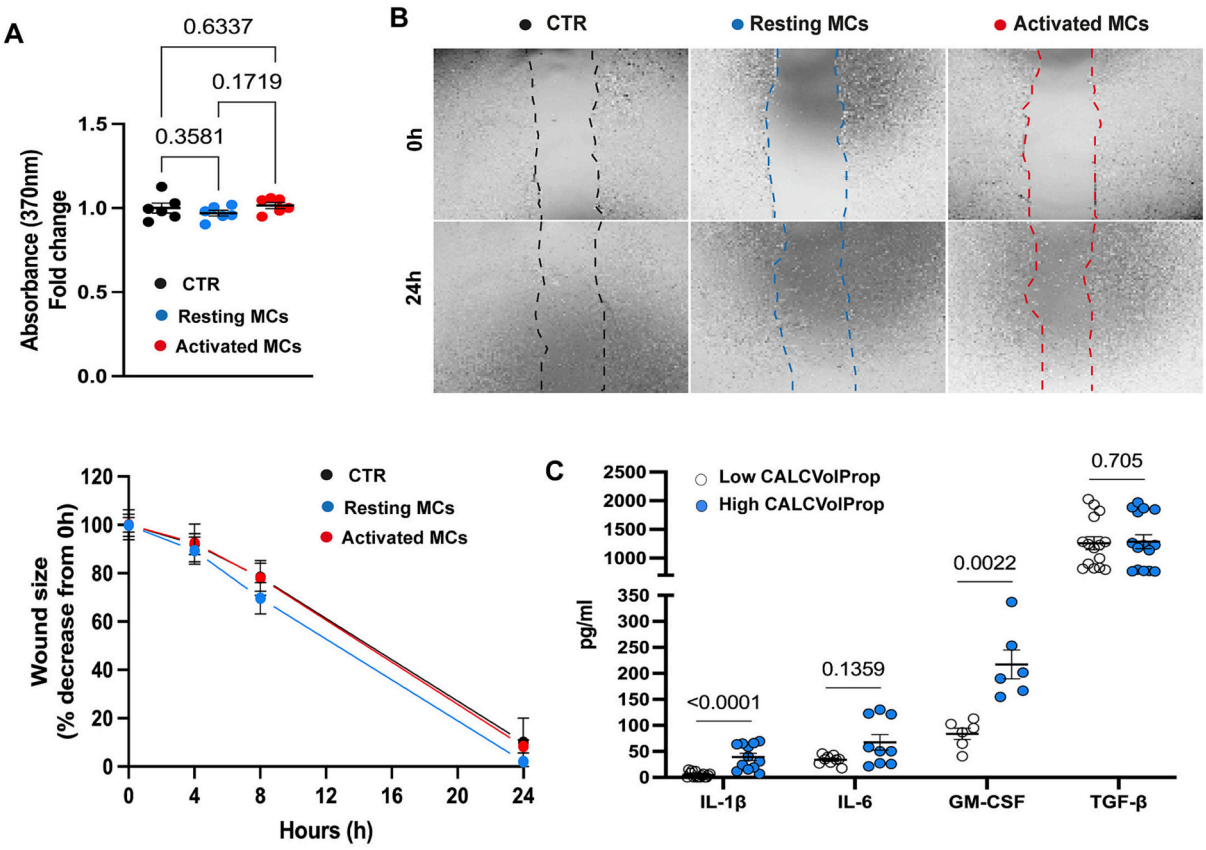

Fig. 6. Functional characterization of HAoSMCs after supplementation with mast cells supernatants.
A) Proliferation assay of HAoSMCs treated with supernatants of resting and activated MCs for 24 h. Statistical significance between groups was assessed by one-way ANOVA multiple comparison test; data expressed as mean with SEM. **B)** Migration scratch assay of HAoSMCs treated with supernatants of resting and activated MCs for 24 h. Statistical significance between groups was assessed by 2-way ANOVA multiple comparison test; data expressed as mean with SEM as percentage of decrease in wound size from time point $t = 0$ h. All experiments performed in biological triplicates. C) Cytokine quantification of IL-1β, IL-6, GM-CSF and TGF-β in the supernatants of low- and high-calcified carotid plaques ($n = 3$ *vs* 3). Several technical replicates were measured from each plaque, all presented individually. Statistical significance between groups was assessed by Mann–Whitney test; data expressed as mean with SEM. Differences between groups were considered significant at P values <0.05.

are further confirmed by immunohistochemistry of the low- and high-calcified plaques, where Tryptase+ MCs were found in proximity of α-SMA/SOX9^{+} SMCs. In addition, our results are in line with the various reported modulatory effects of MCs mediators in bone formation [summarized in Ragipoglu et al. [69]], for example by promoting osteoclastogenesis, osteoblast apoptosis (*e.g.*, histamine, TNF, IL-6) or inhibiting osteoblast activity (*e.g.*, IL-1, TNF), or conversely stimulating osteoblasts (*e.g.*, TGF-β) and reducing osteoclastogenesis (*e.g.*, IL-12, IFN-γ). Exogenous OPN produced by MCs is another mediator that can inhibit the mineralization process by maintaining high levels of pyrophosphate. Among these, we showed that both resting and activated MCs released the highly osteogenic TGF-β1 cytokine, also secreted by both low- and high-calcified plaques (along with *i.e.* IL-1β and GM-CSF), that could promote a synthetic phenotype of SMCs [70,71]. GM-CSF is known to provide an inhibitory signal for MC differentiation and expression of typical MC markers [72,73]. SMCs themselves also exhibited an early upregulation of inflammatory markers, accompanied by IL-1β release in the medium, which were repressed later when ectopic calcification became established. It is already known that IL-1β represses SMC marker gene expression and induces inflammation, proliferation and calcification [74] and could act as a mechanistic driver of the observed phenotypic changes, although this was not reflected on their migro-proliferative capacity. Our results suggest that some of these MC mechanisms already studied in bone formation, could be extrapolated to SMCs osteogenic transdifferentiation in plaques. Moreover, we speculate that it could be a combination of various MC mediators, rather than one single MC-derived factor, that produces these effects. Consequently, the functional synergies between MCs and SMCs could be an important factor in the context of calcification and directly associated with patient symptomatology.

4.1. Limitations and future studies

Our study represents the first comprehensive investigation of MC role in vascular calcification from a large human atherosclerosis cohort and the data warrant further studies to obtain deeper mechanistic insight. For example, as BiKE cohort comprises patients with advanced disease state and late-stage lesions only, the role of MC in disease initiation and progression could be explored in other cohorts. Of note, the CTA analysis was done on the whole lesion, while gene expression microarray analysis was done only on the proximal half of the lesion including the most stenotic part. We acknowledge that inclusion of human MCs into the *in vitro* experiments would have improved the study, however it was not technically feasible. Technical challenges and time constraints have also impeded the collection of more human plaques for *ex vivo* experiments that likely do not capture the full heterogeneity of human atherosclerosis. A more detailed mechanistic examination of the contribution of MCs to SMC transition and matrix mineralization using human plaque material in *ex vivo* studies will be of importance. Lastly, future *in vivo* animal experiments in order to confirm the functional role of MCs in SMC calcification will shed more light on the underlying mechanisms.

5. Conclusions

Our translational approach underpins an engagement of MCs in atherosclerotic intimal calcification, despite being a minor plaque cell type. Activated MCs are abundant in low-calcified plaques with a large necrotic core that give rise to symptoms in patients, while resting MCs are abundant in high-calcified plaques. Both MC populations are capable of inducing SMC transition towards a pro-inflammatory, osteochondrocyte-like phenotype, without modulating their migro-proliferative functions. However, extensive plaque calcification finally inhibits MC activation, supporting our previous BiKE data [9] that macrocalcification provides stabilization for carotid lesions on molecular and cellular level. Based on these results, we propose that the late-stage, already calcified plaque SMCs have a feedback effect on dampening MC activation, which finally outweighs the effects of MCs on inducing SMCs calcification that likely happens earlier during the atheroprogression.

5.1. Translational perspective

Here we applied integrative, systems biology studies from a large human biobank to explore the link between macrocalcification and MC activation in atherosclerotic plaques. Our study is the first to establish a negative association between MC activation and carotid plaque macrocalcification, while positive association with features of plaque vulnerability was confirmed. Interestingly, no beneficial effect of typical medications on the ratio of active *vs.* resting MC populations in plaques could be shown. Mechanistically, both MC populations were capable of inducing SMC osteogenic reprograming and matrix calcification, while calcification in turn attenuated MC activation, offering new intervention points for exploration of MC targeted therapies.

Funding

This work was funded by a research grant from the European Union's Horizon 2020 research and innovation program under the Marie Skłodowska-Curie grant agreement No 722609 (INTRICARE); Ljubica Matic is the recipient of fellowships and awards from the Swedish Research Council [VR, 2019–02027], Swedish Heart-Lung Foundation [HLF, 20210466, 20200621, 20200520, 20180244, 20180247, 201602877], Swedish Society for Medical Research [SSMF, P13-0171]. Ljubica Matic also acknowledges funding from Sven and Ebba-Christina Hagberg, Tore Nilsson's, Magnus Bergvall's and Karolinska Institute research (KI Fonder) and doctoral education (KID) foundations. IB is an Established Investigator of the Dutch Heart Foundation [2019T067].

Author contributions

NTS, EH, LD, GK, EK, IB and LjM performed experiments and data analyses; ML and MK provided technical support; XZ provided bioinformatic support; LM participated in the generation of microarray data, LJS provided material and cells for the study. NTS and LjM conceived and designed the study. NTS, EALB, IB and LjM interpreted the study. IB and LjM supervised the study. NTS and LjM drafted and revised the manuscript with input from all co-authors. HA and LjM provided funding for the study. All authors participated in writing of the manuscript and critical revisions.

Declaration of Competing Interest

The funding bodies and companies were not involved in the study design, manuscript writing or any other involvement in the creation of this manuscript.

Data availability

Data will be made available on request.

Acknowledgements

The Authors acknowledge all staff and surgeons from the Vascular Surgery Unit, Karolinska University Hospital, Sweden. Schematic drawings were created with BioRender (biorender.com).

Appendix A. Supplementary data

Supplementary data to this article can be found online at https://doi.org/10.1016/j.vph.2023.107167.

References

[1] P. Libby, G.K. Hansson, From focal lipid storage to systemic inflammation: JACC review topic of the week, J. Am. Coll. Cardiol. 74 (12) (2019) 1594–1607.
[2] A. Gistera, G.K. Hansson, The immunology of atherosclerosis, Nat. Rev. Nephrol. 13 (6) (2017) 368–380.
[3] A.V. Finn, M. Nakano, J. Narula, F.D. Kolodgie, R. Virmani, Concept of vulnerable/unstable plaque, Arterioscler. Thromb. Vasc. Biol. 30 (7) (2010) 1282–1292.
[4] S.E. New, E. Aikawa, Cardiovascular calcification: an inflammatory disease, Circulat. J. 75 (6) (2011) 1305–1313.
[5] O.J. Waring, N.T. Skenteris, E.A.L. Biessen, M. Donners, Two-faced Janus: the dual role of macrophages in atherosclerotic calcification, Cardiovasc. Res. 118 (13) (2022) 2768–2777.
[6] L. Perisic, S. Aldi, Y. Sun, L. Folkersen, A. Razuvaev, J. Roy, M. Lengquist, S. Akesson, C.E. Wheelock, L. Maegdefessel, A. Gabrielsen, J. Odeberg, G. K. Hansson, G. Paulsson-Berne, U. Hedin, Gene expression signatures, pathways and networks in carotid atherosclerosis, J. Intern. Med. 279 (3) (2016) 293–308.
[7] R.M. Kwee, Systematic review on the association between calcification in carotid plaques and clinical ischemic symptoms, J. Vasc. Surg. 51 (4) (2010) 1015–1025.
[8] L. Saba, W. Brinjikji, J.D. Spence, M. Wintermark, M. Castillo, G.J. de Borst, Q. Yang, C. Yuan, A. Buckler, M. Edjlali, T. Saam, D. Saloner, B.K. Lal, D. Capodanno, J. Sun, N. Balu, R. Naylor, A.V.D. Lugt, B.A. Wasserman, M.E. Kooi, J. Wardlaw, J. Gillard, G. Lanzino, U. Hedin, D. Mikulis, A. Gupta, J.K. DeMarco, C. Hess, J.V. Goethem, T. Hatsukami, P. Rothwell, M.M. Brown, A.R. Moody, Roadmap consensus on carotid artery plaque imaging and impact on therapy strategies and guidelines: an international multispecialty, expert review and position statement, AJNR Am J Neuroradiol 42 (9) (2021) 1566–1575.
[9] E. Karlof, T. Seime, N. Dias, M. Lengquist, A. Witasp, H. Almqvist, M. Kronqvist, J. R. Gadin, J. Odeberg, L. Maegdefessel, P. Stenvinkel, L.P. Matic, U. Hedin, Correlation of computed tomography with carotid plaque transcriptomes associates calcification with lesion-stabilization, Atherosclerosis 288 (2019) 175–185.
[10] Y. Kataoka, K. Wolski, K. Uno, R. Puri, E.M. Tuzcu, S.E. Nissen, S.J. Nicholls, Spotty calcification as a marker of accelerated progression of coronary atherosclerosis: insights from serial intravascular ultrasound, J. Am. Coll. Cardiol. 59 (18) (2012) 1592–1597.
[11] N. Nerlekar, F.J. Ha, C. Cheshire, H. Rashid, J.D. Cameron, D.T. Wong, S. Seneviratne, A.J. Brown, Computed tomographic coronary angiography-derived plaque characteristics predict major adverse cardiovascular events: a systematic review and Meta-analysis, Circulation. Cardiovasc. Imag. 11 (1) (2018), e006973.
[12] E. Aikawa, M. Nahrendorf, J.-L. Figueiredo, K. Swirski Filip, T. Shtatland, H. Kohler Rainer, A. Jaffer Farouc, M. Aikawa, R. Weissleder, Osteogenesis associates with inflammation in early-stage atherosclerosis evaluated by molecular imaging in vivo, Circulation 116 (24) (2007) 2841–2850.
[13] E. Karlof, A. Buckler, M.L. Liljeqvist, M. Lengquist, M. Kronqvist, M.A. Toonsi, L. Maegdefessel, L.P. Matic, U. Hedin, Carotid plaque phenotyping by correlating plaque morphology from computed tomography angiography with transcriptional profiling, Eur. J. Vasc. Endovasc. Surg. 62 (5) (2021) 716–726.
[14] T. Seime, A.C. Akbulut, M.L. Liljeqvist, A. Siika, H. Jin, G. Winski, R.H. van Gorp, E. Karlof, M. Lengquist, A.J. Buckler, M. Kronqvist, O.J. Waring, J.H.N. Lindeman, E.A.L. Biessen, L. Maegdefessel, A. Razuvaev, L.J. Schurgers, U. Hedin, L. Matic, Proteoglycan 4 modulates osteogenic smooth muscle cell differentiation during vascular remodeling and intimal calcification, Cells 10 (6) (2021).
[15] N.T. Skenteris, T. Seime, A. Witasp, E. Karlöf, G.B. Wasilewski, M.A. Heuschkel, A. M.G. Jaminon, L. Oduor, R. Dzhanaev, M. Kronqvist, M. Lengquist, F. Peeters, M. Söderberg, R. Hultgren, J. Roy, L. Maegdefessel, H. Arnardottir, E. Bengtsson, I. Goncalves, T. Quertermous, C. Goettsch, P. Stenvinkel, L.J. Schurgers, L. Matic, Osteomodulin attenuates smooth muscle cell osteogenic transition in vascular calcification, Clin Transl Med 12 (2) (2022), e682.
[16] I. Bot, E.A. Biessen, Mast cells in atherosclerosis, Thromb. Haemost. 106 (5) (2011) 820–826.
[17] P.T. Kovanen, Mast cells as potential accelerators of human atherosclerosis—from early to late lesions, Int. J. Mol. Sci. 20 (18) (2019) 4479.
[18] M. Kaartinen, A. Penttila, P.T. Kovanen, Accumulation of activated mast cells in the shoulder region of human coronary atheroma, the predilection site of atheromatous rupture, Circulation 90 (4) (1994) 1669–1678.

[19] P.T. Kovanen, M. Kaartinen, T. Paavonen, Infiltrates of activated mast cells at the site of coronary atheromatous erosion or rupture in myocardial infarction, Circulation 92 (5) (1995) 1084–1088.

[20] P. Laine, M. Kaartinen, A. Penttila, P. Panula, T. Paavonen, P.T. Kovanen, Association between myocardial infarction and the mast cells in the adventitia of the infarct-related coronary artery, Circulation 99 (3) (1999) 361–369.

[21] M. Kaartinen, A. Penttila, P.T. Kovanen, Mast cells accompany microvessels in human coronary atheromas: implications for intimal neovascularization and hemorrhage, Atherosclerosis 123 (1–2) (1996) 123–131.

[22] H. Lappalainen, P. Laine, M.O. Pentikainen, A. Sajantila, P.T. Kovanen, Mast cells in neovascularized human coronary plaques store and secrete basic fibroblast growth factor, a potent angiogenic mediator, Arterioscler. Thromb. Vasc. Biol. 24 (10) (2004) 1880–1885.

[23] S. Willems, A. Vink, I. Bot, P.H. Quax, G.J. de Borst, J.P. de Vries, S.M. van de Weg, F.L. Moll, J. Kuiper, P.T. Kovanen, D.P. de Kleijn, I.E. Hoefer, G. Pasterkamp, Mast cells in human carotid atherosclerotic plaques are associated with intraplaque microvessel density and the occurrence of future cardiovascular events, Eur. Heart J. 34 (48) (2013) 3699–3706.

[24] I. Bot, S.C. de Jager, A. Zernecke, K.A. Lindstedt, T.J. van Berkel, C. Weber, E. A. Biessen, Perivascular mast cells promote atherogenesis and induce plaque destabilization in apolipoprotein E-deficient mice, Circulation 115 (19) (2007) 2516–2525.

[25] T. Guo, W.Q. Chen, C. Zhang, Y.X. Zhao, Y. Zhang, Chymase activity is closely related with plaque vulnerability in a hamster model of atherosclerosis, Atherosclerosis 207 (1) (2009) 59–67.

[26] M. Jeziorska, C. McCollum, D.E. Woolley, Mast cell distribution, activation, and phenotype in atherosclerotic lesions of human carotid arteries, J. Pathol. 182 (1) (1997) 115–122.

[27] A.R. Naylor, P.M. Rothwell, P.R.F. Bell, Overview of the principal results and secondary analyses from the European and north American randomised trials of endarterectomy for symptomatic carotid stenosis, Eur. J. Vasc. Endovasc. Surg. 26 (2) (2003) 115–129.

[28] A. Halliday, M. Harrison, E. Hayter, X. Kong, A. Mansfield, J. Marro, H. Pan, R. Peto, J. Potter, K. Rahimi, A. Rau, S. Robertson, J. Streifler, D. Thomas, 10-year stroke prevention after successful carotid endarterectomy for asymptomatic stenosis (ACST-1): a multicentre randomised trial, Lancet 376 (9746) (2010) 1074–1084.

[29] L. Perisic Matic, U. Rykaczewska, A. Razuvaev, M. Sabater-Lleal, M. Lengquist, L. Miller Clint, I. Ericsson, S. Röhl, M. Kronqvist, S. Aldi, J. Magné, V. Paloschi, M. Vesterlund, Y. Li, H. Jin, G. Diez Maria, J. Roy, D. Baldassarre, F. Veglia, E. Humphries Steve, U. De Faire, E. Tremoli, N. Null, J. Odeberg, V. Vukojević, J. Lehtiö, L. Maegdefessel, E. Ehrenborg, G. Paulsson-Berne, K. Hansson Göran, H. N. Lindeman Jan, P. Eriksson, T. Quertermous, A. Hamsten, U. Hedin, Phenotypic modulation of smooth muscle cells in atherosclerosis is associated with downregulation of LMOD1, SYNPO2, PDLIM7, PLN, and SYNM, Arterioscl. Thromb. Vasc. Biol. 36 (9) (2016) 1947–1961.

[30] L. Perisic, E. Hedin, A. Razuvaev, M. Lengquist, C. Osterholm, L. Folkersen, P. Gillgren, G. Paulsson-Berne, F. Ponten, J. Odeberg, U. Hedin, Profiling of atherosclerotic lesions by gene and tissue microarrays reveals PCSK6 as a novel protease in unstable carotid atherosclerosis, Arterioscler. Thromb. Vasc. Biol. 33 (10) (2013) 2432–2443.

[31] M. Sheahan, X. Ma, D. Paik, N.A. Obuchowski, S.St. Pierre, W.P. Newman, G. Rae, E.S. Perlman, M. Rosol, J.C. Keith, A.J. Buckler, Atherosclerotic plaque tissue: noninvasive quantitative assessment of characteristics with software-aided measurements from conventional CT angiography, Radiology 286 (2) (2017) 622–631.

[32] M.T. Chrencik, A.A. Khan, L. Luther, L. Anthony, J. Yokemick, J. Patel, J.D. Sorkin, S. Sikdar, B.K. Lal, Quantitative assessment of carotid plaque morphology (geometry and tissue composition) using computed tomography angiography, J. Vasc. Surg. 70 (3) (2019) 858–868.

[33] B.K. Lal, A.A. Khan, V.S. Kashyap, M.T. Chrencik, A. Gupta, A.H. King, J.B. Patel, J. Martinez-Delcid, D. Uceda, S. Desikan, S. Sikdar, J.D. Sorkin, A. Buckler, Computed tomography angiographic biomarkers help identify vulnerable carotid artery plaque, J. Vasc. Surg. 75 (4) (2022) 1311–1322.e3.

[34] A.J. Buckler, E. Karlöf, M. Lengquist, T.C. Gasser, L. Maegdefessel, L.P. Matic, U. Hedin, Virtual Transcriptomics, Arterioscler. Thromb. Vasc. Biol. 41 (5) (2021) 1738–1750.

[35] L.P. Matic, M. Jesus Iglesias, M. Vesterlund, M. Lengquist, M.G. Hong, S. Saieed, L. Sanchez-Rivera, M. Berg, A. Razuvaev, M. Kronqvist, K. Lund, K. Caidahl, P. Gillgren, F. Ponten, M. Uhlen, J.M. Schwenk, G.K. Hansson, G. Paulsson-Berne, E. Fagman, J. Roy, R. Hultgren, G. Bergstrom, J. Lehtio, J. Odeberg, U. Hedin, Novel multiomics profiling of human carotid atherosclerotic plaques and plasma reveals biliverdin reductase b as a marker of intraplaque hemorrhage, JACC Basic Transl Sci 3 (4) (2018) 464–480.

[36] A.M. Newman, C.L. Liu, M.R. Green, A.J. Gentles, W. Feng, Y. Xu, C.D. Hoang, M. Diehn, A.A. Alizadeh, Robust enumeration of cell subsets from tissue expression profiles, Nat. Methods 12 (5) (2015) 453–457.

[37] D.F. Dwyer, N.A. Barrett, K.F. Austen, Expression profiling of constitutive mast cells reveals a unique identity within the immune system, Nat. Immunol. 17 (7) (2016) 878–887.

[38] D.D. Metcalfe, R. Pawankar, S.J. Ackerman, C. Akin, F. Clayton, F.H. Falcone, G. J. Gleich, A.M. Irani, M.W. Johansson, A.D. Klion, K.M. Leiferman, F. Levi-Schaffer, G. Nilsson, Y. Okayama, C. Prussin, J.T. Schroeder, L.B. Schwartz, H.U. Simon, A. F. Walls, M. Triggiani, Biomarkers of the involvement of mast cells, basophils and eosinophils in asthma and allergic diseases, World Allergy Organ J 9 (2016) 7.

[39] B. Mujaj, D. Bos, M. Selwaness, M.J.G. Leening, M. Kavousi, J.J. Wentzel, A. van der Lugt, A. Hofman, B.H. Stricker, M.W. Vernooij, O.H. Franco, Statin use is associated with carotid plaque composition: the Rotterdam study, Int. J. Cardiol. 260 (2018) 213–218.

[40] M. Kaartinen, A. Penttila, P.T. Kovanen, Mast cells of two types differing in neutral protease composition in the human aortic intima. Demonstration of tryptase- and tryptase/chymase-containing mast cells in normal intimas, fatty streaks, and the shoulder region of atheromas, Arterioscler. Thromb. 14 (6) (1994) 966–972.

[41] M.A.C. Depuydt, K.H.M. Prange, L. Slenders, T. Ord, D. Elbersen, A. Boltjes, S.C. A. de Jager, F.W. Asselbergs, G.J. de Borst, E. Aavik, T. Lonnberg, E. Lutgens, C. K. Glass, H.M. den Ruijter, M.U. Kaikkonen, I. Bot, B. Slutter, S.W. van der Laan, S. Yla-Herttuala, M. Mokry, J. Kuiper, M.P.J. de Winther, G. Pasterkamp, Microanatomy of the human atherosclerotic plaque by single-cell transcriptomics, Circ. Res. 127 (11) (2020) 1437–1455.

[42] E. Kritikou, M.A.C. Depuydt, M.R. de Vries, K.E. Mulder, A.M. Govaert, M.D. Smit, J. van Duijn, A.C. Foks, A. Wezel, H.J. Smeets, B. Slutter, P.H.A. Quax, J. Kuiper, I. Bot, Flow cytometry-based characterization of mast cells in human atherosclerosis, Cells 8 (4) (2019).

[43] S. Kraft, M.H. Jouvin, N. Kulkarni, S. Kissing, E.S. Morgan, A.M. Dvorak, B. Schroder, P. Saftig, J.P. Kinet, The tetraspanin CD63 is required for efficient IgE-mediated mast cell degranulation and anaphylaxis, J. Immunol. 191 (6) (2013) 2871–2878 (Baltimore, Md. : 1950).

[44] A.L. Durham, M.Y. Speer, M. Scatena, C.M. Giachelli, C.M. Shanahan, Role of smooth muscle cells in vascular calcification: implications in atherosclerosis and arterial stiffness, Cardiovasc. Res. 114 (4) (2018) 590–600.

[45] Y. Liang, S. Huang, L. Qiao, X. Peng, C. Li, K. Lin, G. Xie, J. Li, L. Lin, Y. Yin, H. Liao, Q. Li, L. Li, Characterization of protein, long noncoding RNA and microRNA signatures in extracellular vesicles derived from resting and degranulated mast cells, J. Extracellular Ves. 9 (1) (2020) 1697583.

[46] J.W. Fischer, S.A. Steitz, P.Y. Johnson, A. Burke, F. Kolodgie, R. Virmani, C. Giachelli, T.N. Wight, Decorin promotes aortic smooth muscle cell calcification and colocalizes to calcified regions in human atherosclerotic lesions, Arterioscler. Thromb. Vasc. Biol. 24 (12) (2004) 2391–2396.

[47] P. Yang, L. Troncone, Z.M. Augur, S.S.J. Kim, M.E. McNeil, P.B. Yu, The role of bone morphogenetic protein signaling in vascular calcification, Bone 141 (2020), 115542.

[48] L. Woodman, S. Siddiqui, G. Cruse, A. Sutcliffe, R. Saunders, D. Kaur, P. Bradding, C. Brightling, Mast cells promote airway smooth muscle cell differentiation via autocrine up-regulation of TGF-beta 1, J. Immunol. 181 (7) (2008) 5001–5007 (Baltimore, Md. : 1950).

[49] M. Zhang, T. Li, Z. Tu, Y. Zhang, X. Wang, D. Zang, D. Xu, Y. Feng, F. He, M. Ni, D. Wang, H. Zhou, Both high glucose and phosphate overload promote senescence-associated calcification of vascular muscle cells, Int. Urol. Nephrol. 54 (10) (2022) 2719–2731.

[50] Y. Chen, X. Zhao, H. Wu, Transcriptional programming in arteriosclerotic disease, Arterioscler. Thromb. Vasc. Biol. 41 (1) (2021) 20–34.

[51] S.A. Steitz, M.Y. Speer, G. Curinga, H.-Y. Yang, P. Haynes, R. Aebersold, T. Schinke, G. Karsenty, C.M. Giachelli, Smooth muscle cell phenotypic transition associated with calcification, Circ. Res. 89 (12) (2001) 1147–1154.

[52] A.B. Alvarez-Palomo, J. Requena-Osete, R. Delgado-Morales, V. Moreno-Manzano, C. Grau-Bove, A.M. Tejera, M.J. Otero, C. Barrot, I. Santos-Barriopedro, A. Vaquero, J. Mezquita-Pla, S. Moran, C.H. Naya, I. Garcia-Martinez, F.V. Perez, M.A. Blasco, M. Esteller, M.J. Edel, A synthetic mRNA cell reprogramming method using CYCLIN D1 promotes DNA repair, generating improved genetically stable human induced pluripotent stem cells, Stem Cells 39 (7) (2021) 866–881.

[53] S. Xu, A.C. Liu, A.I. Gotlieb, Common pathogenic features of atherosclerosis and calcific aortic stenosis: role of transforming growth factor-β, Cardiovasc. Pathol. 19 (4) (2010) 236–247.

[54] J. Shen, M. Zhao, C. Zhang, X. Sun, IL-1β in atherosclerotic vascular calcification: from bench to bedside, Int. J. Biol. Sci. 17 (15) (2021) 4353–4364.

[55] C. Cochain, E. Vafadarnejad, P. Arampatzi, J. Pelisek, H. Winkels, K. Ley, D. Wolf, A.E. Saliba, A. Zernecke, Single-cell RNA-Seq reveals the transcriptional landscape and heterogeneity of aortic macrophages in murine atherosclerosis, Circ. Res. 122 (12) (2018) 1661–1674.

[56] M. Jeziorska, C. McCollum, D.E. Woolley, Calcification in atherosclerotic plaque of human carotid arteries: associations with mast cells and macrophages, J. Pathol. 185 (1) (1998) 10–17.

[57] I. Bot, D.V. Velden, M. Bouwman, M.J. Kroner, J. Kuiper, P.H.A. Quax, M.R. de Vries, Local mast cell activation promotes neovascularization, Cells 9 (3) (2020).

[58] E.R. Mohler, F. Gannon, C. Reynolds, R. Zimmerman, M.G. Keane, F.S. Kaplan, Bone formation and inflammation in cardiac valves, Circulation 103 (11) (2001) 1522–1528.

[59] E. Wypasek, J. Natorska, G. Grudzień, G. Filip, J. Sadowski, A. Undas, Mast cells in human stenotic aortic valves are associated with the severity of stenosis, Inflammation 36 (2) (2013) 449–456.

[60] I. Šteiner, L. Krbal, T. Rozkoš, J. Harrer, J. Laco, Calcific aortic valve stenosis: Immunohistochemical analysis of inflammatory infiltrate, Pathol. Res. Pract. 208 (4) (2012) 231–234.

[61] I. Šteiner, V. Stejskal, P. Žáček, Mast cells in calcific aortic stenosis, Pathol. Res. Pract. 214 (1) (2018) 163–168.

[62] D. Maślińska, M. Laure-Kamionowska, K. Deręgowski, S. Maśliński, Original articleAssociation of mast cells with calcification in the human pineal gland, Folia Neuropathol. 48 (4) (2010).

[63] A. Marzullo, M.M. Ciccone, C. Covelli, G. Serio, D. Ribatti, Macrophages and mast cells are involved in carotid plaque instability, Romanian J. Morphol. Embryol. 52 (3 Suppl) (2011) 981–984.

[64] E.M.P. Lehtonen-Smeds, M. Mäyränpää, P.J. Lindsberg, L. Soinne, E. Saimanen, A. A.J. Järvinen, O. Salonen, O. Carpén, R. Lassila, S. Sarna, M. Kaste, P.T. Kovanen, Carotid plaque mast cells associate with Atherogenic serum lipids, high grade carotid stenosis and symptomatic carotid artery disease, Cerebrovasc. Dis. 19 (5) (2005) 291–301.
[65] K. Nuotio, S.M. Koskinen, L. Mäkitie, J. Tuimala, P. Ijäs, H.M. Heikkilä, J. Saksi, P. Vikatmaa, P. Sorto, S. Kasari, I. Paakkari, H. Silvennoinen, L. Valanne, M. I. Mäyränpää, L. Soinne, P.T. Kovanen, P.J. Lindsberg, Warfarin treatment is associated to increased internal carotid artery calcification, Front. Neurol. 12 (2021).
[66] S. Willems, D. van der Velden, P.H. Quax, G.J. de Borst, J.P. de Vries, F.L. Moll, J. Kuiper, R.E. Toes, S.C. de Jager, D.P. de Kleijn, I.E. Hoefer, G. Pasterkamp, I. Bot, Circulating immunoglobulins are not associated with intraplaque mast cell number and other vulnerable plaque characteristics in patients with carotid artery stenosis, PLoS One 9 (2) (2014), e88984.
[67] P.T. Kovanen, M. Manttari, T. Palosuo, V. Manninen, K. Aho, Prediction of myocardial infarction in dyslipidemic men by elevated levels of immunoglobulin classes A E, and G, but not M, Arch. Intern. Med. 158 (13) (1998) 1434–1439.
[68] D. Tsiantoulas, I. Bot, M. Ozsvar-Kozma, L. Goderle, T. Perkmann, K. Hartvigsen, D. H. Conrad, J. Kuiper, Z. Mallat, C.J. Binder, Increased plasma IgE accelerate atherosclerosis in secreted IgM deficiency, Circ. Res. 120 (1) (2017) 78–84.
[69] D. Ragipoglu, A. Dudeck, M. Haffner-Luntzer, M. Voss, J. Kroner, A. Ignatius, V. Fischer, The role of mast cells in bone metabolism and bone disorders, Front. Immunol. 11 (2020) 163.
[70] V. Sorokin, K. Vickneson, T. Kofidis, C.C. Woo, X.Y. Lin, R. Foo, C.M. Shanahan, Role of vascular smooth muscle cell plasticity and interactions in Vessel Wall inflammation, Front. Immunol. 11 (2020).
[71] M.O.J. Grootaert, M.R. Bennett, Vascular smooth muscle cells in atherosclerosis: time for a re-assessment, Cardiovasc. Res. 117 (11) (2021) 2326–2339.
[72] P. Welker, J. Grabbe, T. Zuberbier, B.M. Henz, GM-CSF downregulates expression of tryptase, fc epsilon RI and histamine in HMC-1 mast cells, Int. Arch. Allergy Immunol. 113 (1–3) (1997) 284–286.
[73] T. Zuberbier, P. Welker, J. Grabbe, B.M. Henz, Effect of granulocyte macrophage colony-stimulating factor in a patient with benign systemic mastocytosis, Br. J. Dermatol. 145 (4) (2001) 661–666.
[74] C. Wen, X. Yang, Z. Yan, M. Zhao, X. Yue, X. Cheng, Z. Zheng, K. Guan, J. Dou, T. Xu, Y. Zhang, T. Song, C. Wei, H. Zhong, Nalp3 inflammasome is activated and required for vascular smooth muscle cell calcification, Int. J. Cardiol. 168 (3) (2013) 2242–2247.